Quantitative Accuracy Assessment and Optimization of SPECT Geometrical Calibration[*]

MA Tianyu (马天予)[**], MIAO Yinbin (缪寅斌), YAO Rutao[†], DAI Tiantian (戴甜甜), DENG Xiao[†]

**Key Laboratory of Particle & Radiation Imaging of Ministry of Education,
Department of Engineering Physics, Tsinghua University, Beijing 100084, China;
† Department of Nuclear Medicine, State University of New York at Buffalo, Buffalo, New York 14214, USA**

Abstract: Accurate geometrical calibration is critical to obtaining high resolution and artifact free reconstructed images for modern animal single photon emission computed tomography (SPECT) systems. Although there have been many published works on the calibration of various SPECT systems, few studies have been done to evaluate the efficacy of the proposed calibration methods in a quantitative manner. This paper presents a numerical method to assess both the uniqueness and the quantitative accuracy of SPECT calibration, which is based on analyzing the singular value decomposition (SVD) components of the Jacobian matrix from a least-square cost function of the calibration. The proposed method is firstly validated by applying it to the calibration of a single pinhole SPECT system and comparing the results with those derived using a published method, and is then used to optimize the calibration setup for a slit-slat SPECT system. With the proposed method, a minimum required number of point source projections to achieve the desired calibration accuracy can be estimated and used as figure-of-merit to evaluate the goodness of a calibration setup. An inverse-square relationship between the calibration accuracy and the number of sampled projections is revealed. Optimal calibration setup is determined through an exhaustive search among all the possibilities of point source arrangements under certain conditions. We demonstrate that for the studied system, the best calibration accuracy is achieved by arranging the point source over the edge of FOV with evenly-spaced angular positions. Point source experiments were conducted to validate the proposed method.

Key words: single photon emission computed tomography (SPECT); geometrical calibration; Jacobian matrix; singular value decomposition (SVD); slit-slat collimator

Introduction

Single photon emission computed tomography (SPECT) geometrical calibration has been an active topic in recent years with the development of high resolution animal SPECT systems and their successful application to molecular imaging area. In order to achieve high resolution and noise free SPECT images, geometrical parameters of the SPECT system have to be known accurately and be modeled in the reconstruction algorithm. There have been numerous studies on SPECT calibration in the last ten years. Most of the studies employed point source(s) or a specially designed phantom. By acquiring tomographic projections through a SPECT scan and fitting the measured data to the analytical models which included those geometrical parameters, optimal estimations of the parameters were obtained. Such methods have proven successful

for providing high quality SPECT images. However, in most of the published approaches, calibration setups were empirically designed, and few studies focused on quantitative analysis of the impact of calibration setups on the estimation accuracy of the parameters.

Presented here is a numerical method to assess the characteristics of both uniqueness and numerical accuracy characteristics of a given geometrical calibration setup. The method is based on analyzing the singular value decomposition (SVD) components of the Jacobian matrix from a least-square cost function of the calibration. With the presented method, we can compare different calibration setups in a quantitative manner and find the optimal one. In this work, the presented method is validated through comparison with published results, and is then applied to a slit-slat SPECT system for calibration setup optimization.

2　Methodology

In this section, we briefly review the proposed SVD-based method for calibration performance analysis. Readers are referred to Ref. [1] for more details.

For a given SPECT system with the calibration parameter set $\boldsymbol{\varGamma}$ to be determined, typically the solution of the calibration problem is found by minimizing the following cost function

$$\boldsymbol{\varGamma}^{\dagger} = \arg\min_{\boldsymbol{\varGamma}} F(\boldsymbol{\varGamma}) \qquad (1)$$

where $F(\boldsymbol{\varGamma})$ measures the difference between the measured and predicted projection centroids of one or multiple point sources. In most cases a least square cost function is used, which can be written as

$$F(\boldsymbol{\varGamma}) = \frac{1}{2}\sum_{i=1}^{m}(p_i(\boldsymbol{\varGamma}) - c_i)^2 \frac{1}{2}\sum_{i=1}^{m} f_i(\boldsymbol{\varGamma})^2 \qquad (2)$$

where i is the projection index, m is the total number of projections, p_i is the predicted projection location of an ideal point source, and c_i is the measured centroid for the measured projection. Ideally c_i is noise-free, and the optimal estimation $\boldsymbol{\varGamma}^*$ that minimizes (2) satisfies $f_i(\boldsymbol{\varGamma}^*) = 0$. When noise e_i exists in c_i, propagation of noise will cause the estimation error

$$\boldsymbol{\varDelta} = \boldsymbol{\varGamma}^{\dagger} - \boldsymbol{\varGamma}^* \qquad (3)$$

where $\boldsymbol{\varGamma}^{\dagger}$ minimizes Eq. (2) with noisy c_i. The corresponding normal equations are

$$\boldsymbol{J}^{\mathrm{T}}\boldsymbol{J}\boldsymbol{\varDelta} = \boldsymbol{J}^{\mathrm{T}}\mathrm{e} \qquad (4)$$

where $\boldsymbol{J}$ is the Jacobian matrix which contains the first partial derivatives of $f_i(\boldsymbol{\varGamma})$. The performance of the calibration problem is analyzed through SVD of $\boldsymbol{J}$. With SVD, the $m \times n$ Jacobian matrix $\boldsymbol{J}$ can be decomposed as

$$\boldsymbol{J} = \boldsymbol{U}\boldsymbol{S}\boldsymbol{V}^{\mathrm{T}} =$$

$$[\boldsymbol{u}_1,\ldots,\boldsymbol{u}_m]\begin{bmatrix} s_1 & & & \\ & s_2 & & \\ & & \ddots & \\ & & & s_n \\ & & 0 & \end{bmatrix}[\boldsymbol{v}_1,\ldots,\boldsymbol{v}_n]^{\mathrm{T}} \qquad (5)$$

where $\boldsymbol{U}$ is an $m \times m$ unitary matrix, $\boldsymbol{S}$ is an $m \times n$ diagonal matrix, and $\boldsymbol{V}$ is an $n \times n$ unitary matrix. $\{\boldsymbol{u}_i\}$, $i = 1,\ldots,m$ and $\{\boldsymbol{v}_j\}, j = 1,\ldots,n$ are called the left-singular and right-singular vectors respectively, and $s_1 \geqslant s_2 \geqslant \cdots \geqslant s_n \geqslant 0$ are the singular values.

The uniqueness condition and quantitative expression of calibration accuracy are described as follows.

(1) Uniqueness condition. The calibration solution is unique when $s_i \neq 0$, $i = 1,\ldots,n$, i.e., $\boldsymbol{J}$ is non-singular. When $\boldsymbol{J}$ is singular, those parameters that have non-zero components in those right singular vectors corresponding to zero singular values cannot be uniquely calibrated.

(2) Calibration accuracy. Suppose e_i can be modeled by independent Gaussian functions with zero mean and same variance σ_c^2, the covariance matrix of estimation error, $\mathrm{cov}(\boldsymbol{\varDelta})$, can be written as

$$\mathrm{cov}(\boldsymbol{\varDelta})_{kl} = \sigma_c^2 \sum_{j=1}^{n} \frac{1}{s_j^2}\boldsymbol{v}_j\boldsymbol{v}_j^{\mathrm{T}} \qquad (6)$$

Therefore, the standard deviation (STD) of the j-th parameter $\sigma_{\varGamma_j}$ is given by the square root of the j-th diagonal element of $\mathrm{cov}(\boldsymbol{\varGamma})$

$$\sigma_{\varGamma_j} = \sigma_c\sqrt{\sum_{r=1}^{n}\left(\frac{V_{jr}}{s_r}\right)^2} \qquad (7)$$

which is determined by $\{s_i\}$ and the j-th row vector of $\boldsymbol{V}$. Equation (7) reveals the quantitative relationship between the calibration accuracy $\sigma_{\varGamma_j}$ and the SVD components of $\boldsymbol{J}$. Since V is unitary, i.e., $\sum_{r=1}^{n}V_{jr}^2 = 1$, Eq. (7) provides an intuitive way to judge the calibration accuracy: if all the s_r are large, or the small singular values s_r are combined with very small V_{jr}, one can expect an accurate estimate of the corresponding parameters. Otherwise the accuracy of the corresponding

parameters may be low.

2 Validation of the SVD-Based Method

2.1 Single pinhole SPECT system

The proposed SVD-based method is applied to a single pinhole SPECT system to analyze the calibration performance. In Ref. [2], the geometry of the SPECT system is characterized by 7 parameters, as illustrated in Table 1. Bequé et al. have derived the minimum required number of point sources to ensure the uniqueness of the calibration problem through analytical derivations. Estimation accuracy is calculated both using an analytical equation derived from a linear system model and through numerical simulations in Ref. [3]. In this work, we have reproduced the same geometrical setup and used the proposed method to predict the uniqueness and accuracy of the calibration problem. In cases of using 1, 2, and 3 rotating point sources, corresponding results are compared in the following paragraphs.

Table 1   Definitions of the 7 parameters that describe the geometry of a single pinhole SPECT system in Refs. [2] and [3]

Symbol	Name	Symbol	Name
f	Focal length	e_u , e_v	Electrical shifts
d	Distance	ϕ	Tilt
m	Mechanical offset	ψ	Twist

2.2 Case I: One point source

With one point source, in addition to the 7 parameters in Table 1, parameters to be calibrated also include the point source's coordinate values (r, α, z) in a cylindrical coordinate system. Bequé et al. showed that only α and ψ could be uniquely determined. In the SVD analysis, the calculated singular values are {922, 842, 755, 64.1, 54.5, 46.0, 0.813, 0.703, 0.000, 0.000}. The last two zero singular values s_9 and s_{10} indicate that the calibration problem is non-unique. The last two singular vectors $\mathbf{v}_9$ and $\mathbf{v}_{10}$ are {0.4330, 0.0000, −0.0209, 0.0255, 0.8638, 0.0216, 0.1027, −0.2331, −0.0011, −0.0000} and {0.1125, −0.0000, 0.1644, −0.0951, 0.2287, 0.0056, −0.4595, 0.8293, 0.0040, 0.0000}, corresponding to $\{r, \alpha, z, f, d, m, e_u, e_v, \phi, \psi\}$ respectively. Only α and ψ do not have non-zero components in $\mathbf{v}_9$ and $\mathbf{v}_{10}$. In other words, only these

two parameters can be uniquely calibrated.

2.3 Case II: Two point sources

In the case of two point sources, Bequé et al. found that when $m \neq 0$, the calibration uniqueness condition was satisfied. Otherwise, the calibration was still non-unique. The SVD-based method shows that when $m \neq 0$, the smallest singular value is 0.577, and when $m = 0$ a zero singular value is found in the SVD results. Conclusions of both methods coincide well in both cases.

2.4 Case III: Three point sources

Both Bequé et al.'s method and the SVD-based method illustrate that using 3 point sources located at known distances from each other is sufficient to calibrate a single pinhole SPECT system as long as a "favorable" point-source spatial arrangement is used. Two optimal setups, opt1 and opt2 are suggested in Ref. [3], and the parameter estimation accuracy is calculated using both an analytical equation derived from a linear system model and through numerical simulations. The results are shown in column "anal" and "sim" for both setups.

   With the SVD method, the smallest singular values for calibration setups opt1 and opt2 are 1.293 and 0.705, respectively, meaning that the calibration uniqueness is satisfied. The accuracy calculated from Eq. (7) is shown in Table 2.

Table 2   Comparison of parameter estimation accuracy with both Bequé's methods (taken from Table 3 in Ref. [3]), and the proposed SVD-based method for opt1 and opt2

Setup		Estimation accuracy						
		f	d	d	e_u	e_v	ϕ	ψ
		mm	mm	mm	mm	mm	deg	deg
opt1	anal	0.210	0.030	0.030	0.230	0.190	0.040	0.010
	sim	0.220	0.030	0.030	0.230	0.200	0.040	0.010
	SVD	0.211	0.029	0.030	0.230	0.188	0.040	0.012
opt2	anal	0.350	0.050	0.030	0.230	0.290	0.050	0.010
	sim	0.350	0.050	0.030	0.230	0.310	0.050	0.010
	SVD	0.349	0.052	0.031	0.235	0.292	0.052	0.012

3 Calibration Optimization of a Slit-Slat SPECT System

3.1 Slit-slat SPECT system

The calibration work was initially motivated by the development of a slit-slat animal SPECT system based

on a microPET scanner[4,5]. So the calibration method developed was naturally tested on this system. Figure 1 illustrates the setup of a collimator insert within the PET detector ring. The PET scanner consists of 4 detector rings and each detector ring has 24 detector blocks. Each detector block consists of a 12×12 array of lutetium oxyorthosilicate (LSO) crystals.
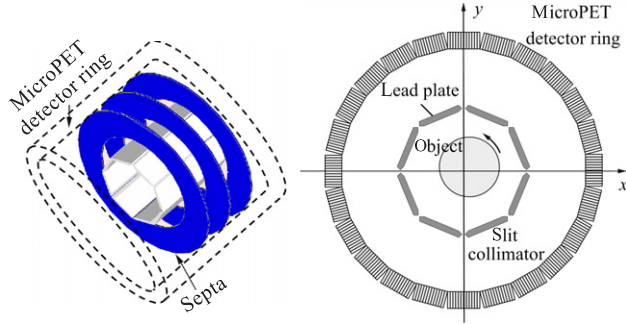
Fig. 1 These two diagrams illustrate the concept of placing a collimator insert inside a PET detector ring for SPECT imaging. The 3-D view on the left shows the relative positioning of the slit-plates and the annular septa (only three septa are shown for clarity). The 2-D transverse view on the right shows the collimator and the detector ring in one plane (septa are not shown).
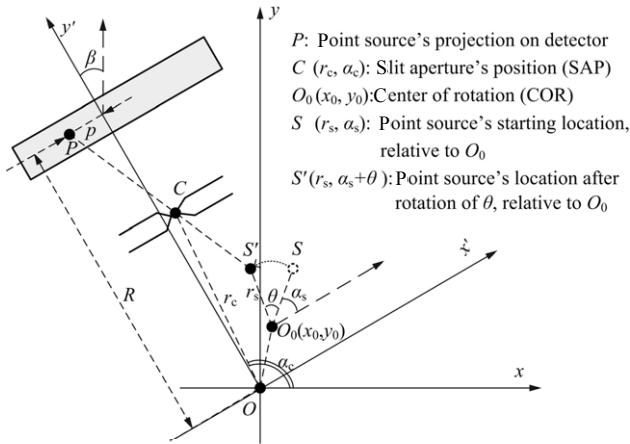
Fig. 2 Geometrical definitions of the coordinate system and the symbols.

For a SPECT system with k slits and when L point sources are used in the calibration, the geometrical parameter set Γ to be calibrated includes:

(1) SAP $(r_{c,k}, \alpha_{c,k})$, where $k = 1, \ldots, K$;

(2) COR $(x_{0,l}, y_{0,l})$, the radius of rotation (ROR) $r_{s,l}$, and the starting angular position of the point source α_{sl}, where $l = 1, \ldots, L$.

3.2 Calibration accuracy comparison with different setup

Five cases of different calibration setups are investigated, as listed below.

- **Case 1** One rotating point source, COR is (0, 0), ROR=17.17 mm.
- **Case 2** One rotating point source, COR is (0, 0), ROR=11.45 mm.
- **Case 3** One rotating point source, COR is (0, 0), ROR=5.72 mm.
- **Case 4** Two rotating point sources, COR are (0, 5.72 mm) and (0, −5.72 mm) respectively, ROR= 11.45 mm.
- **Case 5** Three rotating point sources, COR are (0, 6.28 mm), (5.44 mm, −3.14 mm) and (−5.44 mm, −3.14 mm) respectively, ROR=10.89 mm.

Impact of number of measured projections per point source, N, is investigated first. $N = 60$, 120, 360, 600, 1200, and 3600 are chosen; For each N, the corresponding J, U, S, and V are calculated. The STD of all the parameters are calculated based on Eq. (7). STD(x_0) as a function of N are plotted in Fig. 3 with log-log scale, and are fitted to the following equation

$$\text{STD} = A / \sqrt{N} \qquad (8)$$

where A is a fitting parameter, as shown in Fig. 3.
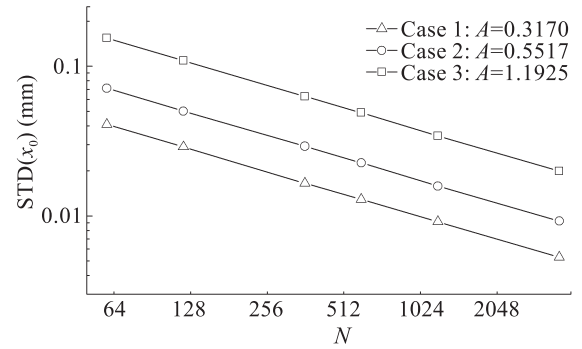
Fig. 3 STD of x_0 are shown as a function of number of projections N for calibration setup cases 1 to 3.

Equation (9) reveals a simple but useful relationship between the calibration accuracy and the number of projection samplings. Theoretical explanation of this relationship can be found in Ref. [6]. Therefore, given a desired calibration accuracy criteria, the minimum required number of projections can be used to judge the goodness of a calibration setup. Table 3 shows the minimum required number of total projections N_P, where N_P is the product of N and the number of point sources used when the specific accuracy criteria is satisfied. It is obvious that Case 1 provides the most favorable accuracy among the studied cases.

Table 3   The minimum number of total projections N_P **required to achieve a desired calibration accuracy for the 5 calibration setup cases.**

Case index	N_P				
	$\sigma_{x_0} <$ 0.017 mm	$\sigma_{y_0} <$ 0.017 mm	$\sigma_{\alpha_s} <$ 0.054°	$\sigma_{r_c} <$ 0.033 mm	$\sigma_{\alpha_c} <$ 0.095°
1	346	346	10	64	21
2	1053	1050	30	180	51
3	4920	4909	140	8090	215
4	745	637	20	126	36
5	658	663	20	123	35

3.3   Optimization of calibration setup

Another investigation is conducted using a fixed

number of measure projections, and exhaustively evaluating all the possible calibration setups to search for the global optimal calibration setup. Figures 4a-4c shows the optimal setup with 3, 4, and 5 projections among all the possible combinations when the point source is placed onto the cross points of a 11×11 grid. The size of the grid is about the same as for an FOV. It is found that in all cases the point sources have to be located over the edge of the FOV to provide optimal calibration accuracy.

We also investigated the optimal setup using 7 projections, by constraining the location of point sources to be on the "edge circle" of the FOV. As shown in Fig. 4d, the 7 projections are roughly evenly spaced over the edge circle.

Fig. 4   Global optimal calibration setup with (a) 3 projections, (b) 4 projections and (c) 5 projections, when the point source is placed in the cross point of the 11×11 grid. (d) Optimal calibration setup with 7 projections are constrained to be in the red circle.

4   Experimental Studies

Point source experiments were conducted to test the calibration accuracy and validate the proposed methods. A ^{57}Co point source was used to acquire the

SPECT data for calibration. By mounting the point source onto the same rotation stage, two groups of SPECT data were acquired, the COR were the same and the ROR were 15.47 mm (Orbit A) and 6.02 mm (Orbit B). For each orbit, 360 projections were

acquired with $3°$/step. By selecting only a portion of the projections, impact of N on the calibration accuracy can be investigated. 7 different choices of $N = 40$, 45, 60, 90, 120, 180, and 360 were used, and the selected projections were always evenly spaced over $360°$. For each N, the acquired list mode data were evenly split into 100 pieces to generate 100 realizations of measured projections. Therefore, the calibration was repeated $7×100$ times. For each N, $STD(x_0)$ were calculated over the 100 realizations and the results are shown in Fig. 5. Similar to Fig. 3, a linear shape is observed in the log-log scale plot for both curves. By fitting the data to

$$STD = AN^B \qquad (9)$$

It is found that $B = -0.512$ for Orbit A and $B = -0.510$ for Orbit B. The result coincides well with Eq. (9). Figure 5 also shows that Orbit A provides better estimation accuracy than Orbit B.
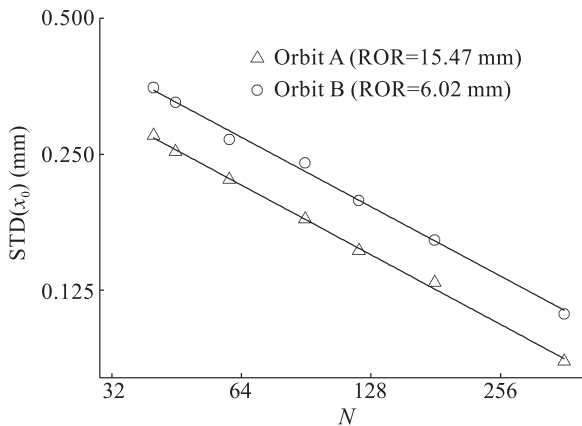
Fig. 5 STD of x_0 are shown as a function of the number of projections N

5 Conclusions

In this work, an SVD-based numerical method is used to analyze the quantitative accuracy of SPECT calibration. By applying the method to a slit-slat SPECT system, conditions for optimizing the calibration setup are studied in terms of using the smallest number of point source measurements to achieve the desired calibration accuracy. According to the optimization study results, it is suggested that the point source(s) should be placed as close to the edge of the FOV as possible and with evenly-spaced angular positions. An inverse-square relationship between the calibration accuracy and the number of point source measurements is observed both in numerical calculations and in calibration experiments, which is explained by a theorem in nonlinear regression theory. Calibration optimization studies with limited number of projections are conducted through an exhaustive searching approach. In the studied system, it is suggested to that the point source measuring locations be uniformly arranged on the edge of the FOV to reach optimal calibration accuracy.

References

[1] Ma T, Yao R, Shao Y. A SVD-based method to assess the uniqueness and accuracy of SPECT geometrical calibration. *IEEE Trans. Med. Imag.*, 2009, **28**(2): 1929-1939.

[2] Beque D, Nuyts J, Bormans G, et al. Characterization of pinhole SPECT acquisition geometry. *IEEE Trans. Med. Imag.*, 2003, **22**(5): 599-612.

[3] Beque D, Nuyts J, Suetens P, et al. Optimization of geometrical calibration in pinhole SPECT. *IEEE Trans. Med. Imag.*, 2005, **24**(2): 180-190.

[4] Shao Y, Yao R, Ma T, et al. Initial studies of PET-SPECT dual-tracer imaging. In: Rec. IEEE 2007 Nucl. Sci. Symp. Med. Imag. Conf. 2007, **6**: 4198-4204.

[5] Yao R, Ma T, Shao Y. Lutetium oxyorthosilicate (LSO) intrinsic activity correction and minimal detectable target activity study for SPECT imaging with a lso-based animal PET scanner. *Phys. Med. Biol.*, 2008, **53**(16): 4399-4415.

[6] Gallant R A. Testing a subset of the parameters of a nonlinear regression model. *J. Am. Stat. Assoc.*, 1975, **70**(352): 927-932.